Simulation of friction in nanoconfined fluids for an arbitrarily low shear rate

Jerome Delhommelle and Peter T. Cummings
Department of Chemical Engineering, Vanderbilt University, 118 Olin Hall, Nashville, Tennessee 37235-1604
(Received 13 June 2005; published 29 November 2005)

Molecular dynamics (MD) simulations are a valuable tool to characterize the microscopic mechanisms underlying friction. However, the lowest shear rate accessible by current MD methods is at least four orders of magnitude larger than those typically used in experiments. Using the transient-time correlation function, we show how MD simulations can be extended to study systems subjected to a realistic shear rate. We demonstrate the usefulness of this approach by studying the frictional response of a simple fluid confined to a film of about five molecular diameters.

DOI: 10.1103/PhysRevB.72.172201 PACS number(s): 66.20.+d, 02.70.Ns, 81.40.Pq

Friction is an extremely complex phenomenon, common to many technological, geological, and biological applications. To understand friction, one needs to be able to characterize what is going on the "single asperity" level, i.e., at the molecular level.[1] Experiments using the surface forces apparatus (SFA),[2] which monitor the frictional response of a fluid confined between smooth mica sheets, play a key role in identifying the microscopic mechanisms underlying this phenomenon. Atomistic molecular dynamics (MD) simulations provide another route to analyze this phenomenon at the molecular level. Early MD studies on model systems have helped us to understand liquid layering under nanoconfinment[3] and the nature of transitions between "smooth" and stick-slip sliding.[4] Since then, accurate force fields for the mica sheets and the confined fluid have been developed. This opened the door to realistic simulations of the SFA experiment. MD studies were recently carried out for confined water[5] and confined dodecane[6] under shear. The results so obtained were consistent with experimental findings. However, a direct comparison between simulation and experiment still remains impossible. This is because the lowest shear rates accessible by MD are at least four orders of magnitude larger than those typically used in experiments. This limitation directly stems from the MD method. In MD simulations, properties are averaged over the steady state, which becomes very noisy for low shear rates. Having a large signal-to-noise ratio (and hence subjecting the fluid to large shear rates) is therefore crucial to obtain meaningful averages in the steady state. This basically prevents accessing the frictional response for realistic shear rates. Current MD methods are therefore unable to shed light on a number of recent experimental measurements on films of about 5–8 molecular layers. Does the viscosity of organic solvents diverge at such narrow confinement as these fluids undergo freezing?[7,8] Is the efficiency of water-based lubricants, ubiquitous in biological systems, related to the specific properties of nanoconfined water, whose viscosity under those conditions is less than three times its value for the bulk?[9] Does this discrepancy only result from different experimental protocols and should all the fluids actually have similar rheological responses when nanoconfined?[10]

In this work, we address the inability of current MD methods to study nanoconfined liquids subjected to low (realistic) shear rates. We apply a nonlinear generalization of the Green-Kubo relations, the so-called transient time correlation function (TTCF) formalism[11–14] and demonstrate that this approach allows to study the rheological response of a confined fluid subjected to an arbitrarily low shear rate. TTCF gives an exact relation between the nonlinear steady-state response and the so-called transient time correlation function. We briefly outline the general derivation proposed by Evans and Morriss[11] to show how it can be applied to fluids (either in the bulk phase or nanoconfined) undergoing shear flow. Let us consider a phase variable $B(\Gamma)$, where Γ denotes a phase space point. In the Heisenberg representation, the average of B at time t is $\langle B(t)\rangle = \int d\Gamma f(0) B(\Gamma;t)$, where $f(0)$ is the initial distribution function. If we differentiate this expression with respect to time, we obtain, for time-independent external fields

$$\frac{d\langle B(t)\rangle}{dt} = \int d\Gamma f(0) \frac{d\Gamma}{dt} \cdot \frac{\partial B(t)}{\partial \Gamma}. \tag{1}$$

By integrating by parts and realizing that the boundary term vanishes in periodic systems,[11] we see that

$$\frac{d\langle B(t)\rangle}{dt} = -\int d\Gamma B(t) \frac{\partial}{\partial \Gamma} \cdot \frac{d\Gamma}{dt} f(0). \tag{2}$$

Finally, integrating with respect to time, we obtain the nonlinear nonequilibrium response

$$\langle B(t)\rangle = \langle B(0)\rangle - \int_0^t ds \int d\Gamma B(s) \frac{\partial}{\partial \Gamma} \cdot \frac{d\Gamma}{dt} f(0). \tag{3}$$

We now need to specify the equations of motion for the system. The nonequilibrium MD method used in all the studies of simple liquids employs homogeneous shear fields in the so-called SLLOD equations of motion[11] together with appropriate periodic boundary conditions.[15] This method correctly describes an isolated bulk system under arbitrarily strong shear.[11] For a fluid undergoing Couette flow in the x direction with a velocity gradient along the y direction, the SLLOD equations for a particle i are as follows:

$$\dot{\mathbf{r}}_i = \frac{\mathbf{p}_i}{m} + \dot{\gamma} y_i \mathbf{e}_x,$$

$$\dot{\mathbf{p}}_i = \mathbf{F}_i - \dot{\gamma} p_{y_i} \mathbf{e}_x, \tag{4}$$

where $\dot{\gamma}$ denotes the shear rate, m the mass of the particle, and $\mathbf{e}_x$ is an unit vector colinear to the x axis. Applying the SLLOD equations of motion is actually equivalent to (i) initially superimposing the appropriate linear velocity profile to the actual velocities of the molecules of the fluid and (ii) afterwards applying Newton's equations of motion to this fluid. The internal energy is defined as $H_0(\Gamma) = \Sigma_i \mathbf{p}_i^2/(2m) + \phi(\mathbf{q}_i)$. The rate of change in internal energy due to shear is equal to $\dot{H}_0 = -\dot{\gamma} V P_{xy}$, where $P_{xy} = \Sigma_i (p_{xi} p_{yi}/m + F_{xi} y_i)/V$ is the opposite of the shear stress and V the volume of the system. Adiabatic shearing causes a monotonic increase in internal energy. The system heats up and there is no well-defined final steady state from which transport coefficients can be calculated. In reality, viscous heat is dissipated to the environment through container walls, which are omitted in simulations of the bulk. Constant temperature in MD simulations is achieved by adding a "thermostat term" to the equations of motion. If the initial distribution is canonical and if the dynamics of the system follows the SLLOD equations, then, to the first order in the number of particles,[11]

$$(\partial/\partial\Gamma) \cdot [f(0) d\Gamma/dt] = -\dot{H}_0 f(0)/(k_B T) = \dot{\gamma} V P_{xy} f(0)/(k_B T). \tag{5}$$

The average of B at time t is equal to

$$\langle B(t) \rangle = \langle B(0) \rangle - \frac{V\dot{\gamma}}{k_B T} \int_0^t \langle B(s) \cdot P_{xy}(0) \rangle ds. \tag{6}$$

If we choose $B(t) = P_{xy}(t)$, the equilibrium average $\langle P_{xy}(0) \rangle$ is equal to 0 and we obtain the following expression for $\langle P_{xy}(t) \rangle$:

$$\langle P_{xy}(t) \rangle = -\frac{V\dot{\gamma}}{k_B T} \int_0^t \langle P_{xy}(s) \cdot P_{xy}(0) \rangle ds. \tag{7}$$

We now present how TTCF can be applied to a nanoconfined fluid. Let us consider a fluid confined between two walls, separated from each other by a distance L along the y axis. We consider as a starting point ($t=0$) for our study a configuration of the system at equilibrium. At time $t=0^+$, the two walls are driven at a constant velocity, equal to $v/2$, in opposite directions. The fluid particles obey at all times Newton's equations of motion, supplemented by a "thermostat term." Unlike for the bulk, shear does not appear explicitly in the equations of motion: it is induced by the two moving walls. A sketch of the system is presented in Fig. 1. The confined fluid is therefore subjected to a shear rate of v/L. The rate of change of internal energy $\dot{H}_0$ due to shear is equal to $-(v/L) P_{xy} V$ for the confined fluid. The value of the shear stress $-P_{xy}(t)$ is equal to $-\Delta F_x(t)/(2S)$, where S is the surface of a wall. $\Delta F_x(t)$ is the projection on the x axis of the difference between the forces exerted by the fluid on the top wall and on the bottom wall, respectively. Using Eqs. (3) and (5) and substituting $\Delta F_x(t)/(2S)$ for $P_{xy}(t)$, we obtain

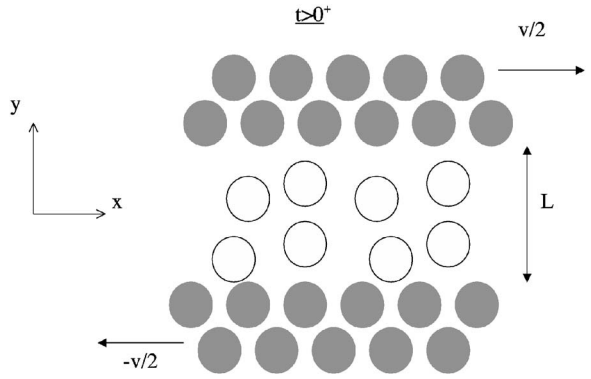

FIG. 1. Projection on the x-y plane of the simulated system. Filled circles stand for wall atoms while open circles represent fluid atoms.

$$\langle P_{xy}(t) \rangle = -\frac{vV}{4 k_B T L S^2} \int_0^t \langle \Delta F(s) \cdot \Delta F(0) \rangle ds. \tag{8}$$

This expression coincides with that recently obtained by Petravic and Harrowell, who applied linear response theory to evaluate the viscosity of a confined fluid.[16]

We apply TTCF to evaluate the viscosity of a simple liquid in the bulk and when confined to a film of about five molecular diameters. Wall and fluid particles are identical and interact with each other through a Weeks-Chandler-Andersen potential ($\phi(r) = -4\varepsilon[(\sigma/r)^6 - (\sigma/r)^{12}] + \varepsilon$ for $r < 2^{1/6}$ and 0 otherwise). In the rest of the paper, we use a system of reduced units, in which σ is the unit of length, ε the unit of energy and m is the unit of mass. Simulations were carried out at constant volume and constant temperature. Temperature control is achieved through the use of a configurational thermostat. This thermostat, which does not require making any assumption about the flow profile, is especially well suited for the study of inhomogeneous systems.[17,18] We study the bulk liquid at a temperature $T = 0.75$ and a number density $n = 0.84$, which corresponds to a state point close to the triple point. The equilibrium pressure for this state point is 6.4. In order to simulate the confined fluid at the same state point, we adjusted the thickness of the film to 5.43 so that the parallel pressure $(P_{xx} + P_{zz})/2$ in the confined fluid is equal to 6.4 and matches that of the bulk liquid (the resulting density for the confined fluid is 0.8408). Simulations are carried out on systems of 250 atoms for the bulk liquid and 490 atoms for the confined fluid. Each wall is two layers thick and there are 98 atoms in each layer. The wall atoms are rigidly fixed to the lattice sites of the (111) face for a fcc structure. The equations of motion were integrated with a fourth-order Runge-Kutta method and a time step of 5×10^{-4}. Using a self-starting method to integrate the equations of motion is absolutely essential in studies of the transient response. For both the bulk and the confined fluid, we generated 30×10^5 equilibrium configurations which served as starting points for the nonequilibrium trajectories (these equilibrium configurations were selected, every 2.5 time units, over the course of a single equilibrium trajectory). Following Evans and Morriss,[11] we used phase-space map-

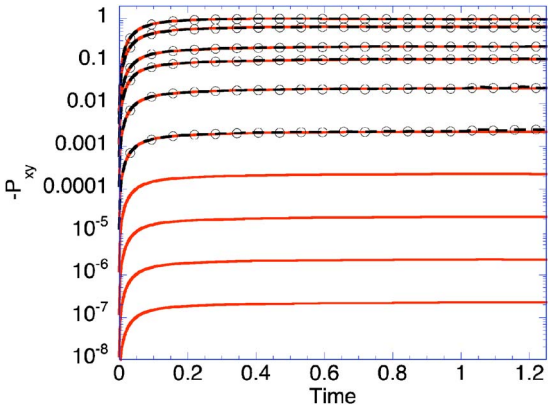

FIG. 2. (Color online) Evolution of shear stress in the bulk with time obtained from TTCF (solid lines) or from an average over all trajectories (dashed lines with circles). The applied shear rate is equal to 1×10^{-7} (bottom curve), 1×10^{-6}, 1×10^{-5}, 1×10^{-4}, 1×10^{-3}, 0.01, 0.05, 0.1, 0.3, and 0.5 (top curve).

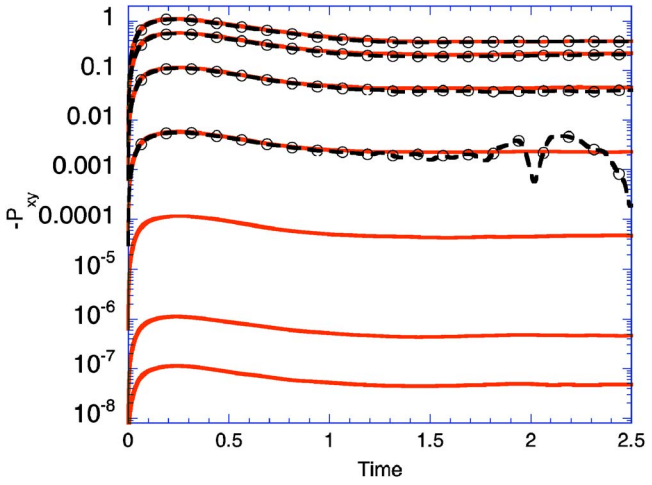

FIG. 3. (Color online) Evolution of shear stress in the confined fluid with time obtained from TTCF (solid lines) or from an average over all trajectories (dashed lines with circles). v is equal to 1×10^{-7} (bottom curve), 1×10^{-6}, 1×10^{-4}, 5×10^{-3}, 0.1, 0.5, and 1 (top curve). The value for the shear rate can be obtained by dividing v by $L=5.43$.

pings of the initial phases in order to improve the statistical reliability of the results and to reduce the number of equilibrium configurations/independent starting points required. For the bulk, we used the four following mappings: the identity mapping $(x,y,z,p_x,p_y,p_z)\rightarrow(x,y,z,p_x,p_y,p_z)$, the time reversal mapping $(x,y,z,p_x,p_y,p_z)\rightarrow(x,y,z,-p_x,-p_y,-p_z)$, the y-reflection mapping $(x,y,z,p_x,p_y,p_z)\rightarrow(x,-y,z,p_x,-p_y,p_z)$, and the Kawasaki mapping, which is the combined effect of time reversal and y-reflection mappings, i.e., $(x,y,z,p_x,p_y,p_z)\rightarrow(x,-y,z,-p_x,p_y,-p_z)$. For the confined fluid, we also used four similar mappings in which the y-reflection mapping was replaced by the x-reflection mapping. This is because, for the confined fluid, applying the y-reflection mapping does not have any effect on the value of P_{xy}. This arises from the fact that we measure the projection of the force along the x axis in order to determine P_{xy}. Thus, applying the x-reflection mapping will have the desired result, i.e., reverse the sign for the value of P_{xy}. In effect, phase-space mappings ensure that $\langle P_{xy}(0)\rangle$ is exactly zero. They also allow one to obtain four different nonequilibrium trajectories for every single equilibrium configuration/starting point. In all cases, TTCF averages were therefore estimated over 1.2×10^5 nonequilibrium trajectories.

We plot in Figs. 2 and 3 the variations of the shear stress, estimated from Eqs. (7) and (8), with time in the bulk and in the confined fluid respectively, for shear rates ranging from 2×10^{-8} to 0.5. If the WCA particles are meant to represent a molecule like water, the shear rates simulated here range from approximately 10^3 to 10^{11} s^{-1}. For all shear rates investigated, the shear stress reaches a plateau after a transient time of 0.6 for the bulk and a transient time of 2 for the confined fluid. The difference between the two transient times mainly results form the difference in the simulation method. For the bulk, at $t=0$, a linear flow profile is added to the equilibrium velocity of each particle and the relaxation starts from this state at $t=0^+$. For the confined fluid, at $t=0$, the velocity of each particle is its equilibrium velocity and shear is induced by the moving walls at $t=0^+$. The initial state is therefore much closer to the steady state in the case of the bulk than in the case of the confined fluid.

Figures 2 and 3 also show a comparison, for shear rates larger than or equal to 10^{-3}, between the TTCF estimates for the shear stress and a direct average of the shear stress, performed over all 1.2×10^5 nonequilibrium trajectories. The results are in excellent agreement for both the bulk and the confined fluid, provided that the shear rate is larger than 10^{-3}. This proves the validity of Eqs. (7) and (8). As the shear rate gets close to 10^{-3}, the direct average exhibits larger fluctuations and the uncertainty in the determination of the steady state average steeply rises. This is best seen in the case of the confined fluid for $v=5\times10^{-3}$ (which corresponds to a shear rate of 10^{-3}) as the behavior of the direct average for the shear stress becomes erratic in the steady state. This shows that for a shear rate of 10^{-3}, there is already too much noise to obtain a reliable steady state average for the shear stress and hence the viscosity. On the contrary, TTCF estimates remain reliable, regardless of how weak the signal-to-noise ratio is.

By dividing the value obtained in the plateau for the shear stress by the shear rate, we can estimate the value of the shear viscosity for the bulk and for the confined fluid. The shear viscosity so obtained is plotted in Fig. 4. For both systems, the viscosity is found to reach a plateau at low shear rates. The viscosity remains constant for shear rates smaller than 0.1 in the case of the bulk and for shear rates smaller than 0.001 in the case of the confined fluid. The value in the Newtonian plateau is equal to 2.22 ± 0.1 for the bulk and to 2.58 ± 0.1 for the confined fluid. These results are in agreement with our expectations. Confined fluids have longer relaxation times. Therefore, the transition from Newtonian to non-Newtonian occurs at a lower shear rate than for the bulk and the viscosity of the confined fluid is larger. For large shear rates, both the bulk and the confined fluid exhibit a shear-thinning regime. To further assess the reliability of the TTCF approach, we checked that the TTCF estimates for the

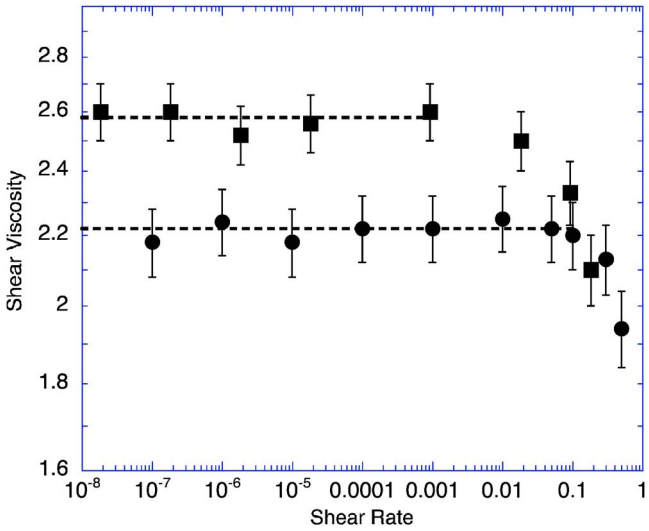

FIG. 4. (Color online) Variations of shear viscosity with the applied shear for the bulk (circles) and for the confined fluid (squares). Dashed lines indicate the Newtonian plateau in both cases.

shear viscosity were in good agreement those obtained with the standard method from the steady state average of the shear stress. As indicated earlier, such a comparison can only be drawn at large shear rates. Even for a simple fluid confined to a film of 5.43 molecular diameters, the standard method is unable to locate the onset of the Newtonian plateau (as shown on Fig. 3, there is already too much noise in the steady state for a wall velocity of 5×10^{-3} shear rate of 10^{-3}). This demonstrates the usefulness of the TTCF approach.

Using TTCF, we have been able to devise a simulation method to study the response of a confined fluid subjected to realistic shear rates. Up to now, simulations of confined fluids under shear were limited to shear rates several orders of magnitude larger than the experimental shear rates. This method allows for a direct comparison between MD and experiments and therefore, greatly improves the relevance of nonequilibrium MD findings. We have been able to show that, even on a simple fluid, TTCF allows us to access the whole range of rheological responses. TTTCF should be particularly helpful in understanding the frictional response of more complex molecules such as oil-based lubricants, which have longer relaxation times and whose rheology at realistic shear rates is currently inaccessible[6] (note, however, that the relaxation time of the confined lubricant has to remain within the time scales accessible by MD simulations). Finally, we add that TTCF is a very general formalism and can be applied to study a system subjected to any kind of perturbation such as, for instance, an electric field.[19]

This work is supported by the National Science Foundation NER/CTS/PMP-0404125.

[1] M. Urbakh, J. Klafter, D. Gourdon, and J. Israelachvili, Nature (London) **430**, 525 (2004).
[2] J. N. Israelachvili and G. E. Adams, J. Chem. Soc., Faraday Trans. **74**, 975 (1978).
[3] J. Gao, W. D. Luedtke, and U. Landman, Phys. Rev. Lett. **79**, 705 (1997).
[4] P. A. Thompson and M. O. Robbins, Science **250**, 792 (1990).
[5] Y. Leng and P. T. Cummings, Phys. Rev. Lett. **94**, 026101 (2005).
[6] S. T. Cui, C. McCabe, P. T. Cummings, and H. D. Cochran, J. Chem. Phys. **118**, 8941 (2003).
[7] S. Granick, Science **253**, 1374 (1991).
[8] J. Klein and E. Kumacheva, J. Chem. Phys. **108**, 6996 (1998).
[9] U. Raviv, P. Laurat, and J. Klein, Nature (London) **413**, 51 (2001).
[10] Y. Zhu and S. Granick, Phys. Rev. Lett. **93**, 096101 (2004).
[11] D. J. Evans and G. P. Morriss, *Statistical Mechanics of Nonequilibrium Liquids* (Academic Press, London, 1990).
[12] W. M. Visscher, Phys. Rev. A **10**, 2461 (1974).
[13] J. W. Dufty and M. J. Lidenfeld, J. Stat. Phys. **20**, 259 (1979).
[14] E. G. D. Cohen, Physica A **118**, 17 (1983).
[15] A. W. Lees and S. F. Edwards, J. Phys. C **5**, 1921 (1972).
[16] J. Petravic and P. Harrowell, Phys. Rev. E **71**, 061201 (2005).
[17] J. Delhommelle, J. Petravic, and D. J. Evans, J. Chem. Phys. **119**, 11005 (2003).
[18] J. Delhommelle, Phys. Rev. B **69**, 144117 (2004).
[19] J. Delhommelle, P. T. Cummings, and J. Petravic, J. Chem. Phys. **123**, 114505 (2005).